Proceedings of the 17th World Congress
The International Federation of Automatic Control
Seoul, Korea, July 6-11, 2008

Robust Control for Output Voltage Across Load of DC-DC Converter Matching with Remote Sensing

E. Takegami*, K. Higuchi **, K. Nakano, T. Kajikawa****

**DENSEI-LAMBDA K.K., 2701 Togawa, Settaya, Nagaoka 940-1195, Japan (Tel: +81-258-22-3663; e-mail: e.takegami@densei-lambda.com)*
*** Dept. of Electronic Engineering, The University of Electro-Communications, 1-5-1 Chofu-ga-oka, Chofu, Tokyo 182-8585, Japan(Tel: +81-42-443-5182; e-mail: higuchi@ee.uec.ac.jp, nakano@ee.uec.ac.jp, kajikawa@ee.uec.ac.jp)*

Abstract: If the lines which connect the output terminal of DC-DC converter and the load are long, the voltage actually across load will be changed largely to produce the voltage drops by the impedances of the lines. Then, the terminal which senses the voltage across load is prepared apart from the output terminal of DC-DC converter, and it leads to the load, and the voltage across load is adjusted so that it is not changed largely. This method is called remote sensing. When the lines becomes long, the usual method of adjusting the voltage across load cannot suppress enough the change of it. In this paper, the robust digital controller for suppressing the change of the voltage across load is proposed. Experimental studies using DSP demonstrate that this type of digital controller is effective to suppress it.

1. INTRODUCTION

If the lines which connect the output terminal of DC-DC converter and the load are long, the voltage actually across load will be changed largely in order to produce voltage drops by the impedances of the lines. Then, the terminal which senses the voltage across load is prepared apart from the output terminal of DC-DC converter, and it leads to the load, and the voltage across load is adjusted so that it is not changed largely. This method is called remote sensing. At remote sensing, usual simple integral control etc. of 1-degree-of-freedom (Guo *et al*., 2003) are performed. When the lines becomes long, the usual method of adjusting the voltage across load cannot suppress enough the change of it. In this paper, as a controller for adjusting the voltage across load, the robust digital controller using the approximation 2-degree-of-freedom (2DOF) method is proposed. By this method, even if the lines are long or short, the change of the voltage across load can be suppressed enough. When the lines long, it is necessary to design the controller in consideration of the sizes of the inductances. The authors proposed previously the robust digital controller when using LC filter as the noise removal filter of DC-DC converter (Higuchi *et al*., 2004, 2005). At remote sensing, the inductances of the lines must also be taken into consideration and it must be assumed that LCLC filter is connected. The method of designing an approximated 2-degree-of-freedom robust controller when LCLC filter is connected to DC-DC converter is shown. Because of robust controller the output voltage change can be suppressed also at remote sensing, without changing the controller at non-remote sensing. This controller is actually implemented on a DSP and is connected to a DC-DC converter. Experimental studies demonstrate that the digital controller designed by the proposed method can suppress enough the change of the voltage across load having no relation of the length of the lines.

2. RESPONSE CHRACTERITICS FOR CONTROLLED OBJEC T

2.1 Linearization of model for controlled object

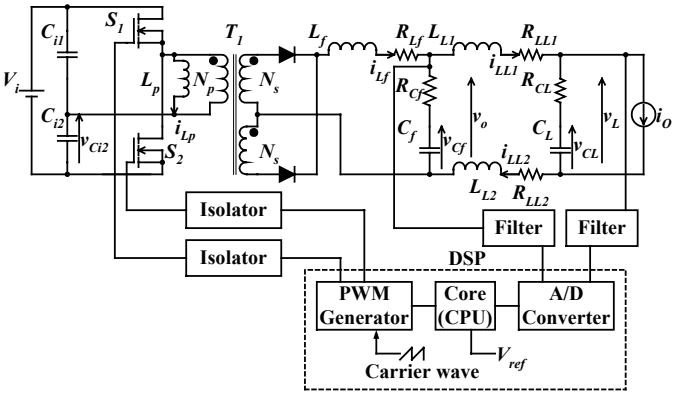

Fig. 1. DC-DC converter

A DC-DC converter is shown in Fig. 1. In Fig.1, V_i is input voltage, C_{i1} and C_{i2} are input capacitances, S_1 and S_2 are main switches, L_f and R_{Lf} are output inductance and equivalent series resistance, T_1 is transformer and N_p and N_s are the numbers of turns. L_{L1}, L_{L2} and R_{LL1}, R_{LL2} are inductances and resistances of the lines. C_L and R_{CL} are capacitance and equivalent series resistance by the side of load and i_o is load current. Here, if $C_{i1} + C_{i2}$ is large enough, it is considered as the constant voltage supply and if L_p is also large enough, it will be disregarded. Then, the linear

model shown in Fig. 2 will be obtained. And the state equation becomes as follows (Fukuda *et al*., 1993):

$$\begin{aligned} \dot{x} &= A_C x + B_C u \\ y &= Cx + Du \end{aligned} \tag{1}$$

where

$$A_C = \begin{bmatrix} 0 & \frac{1}{C_L} & 0 & 0 \\ -\frac{1}{L_L} & -\frac{R_{CL}+R_{LL}+R_{Cf}}{L_L} & \frac{1}{L_L} & \frac{R_{Cf}}{L_L} \\ 0 & -\frac{1}{C_f} & 0 & \frac{1}{C_f} \\ 0 & \frac{R_{Cf}}{L_f} & -\frac{1}{L_f} & -\frac{R_{Cf}+R_{Lf}}{L_f} \end{bmatrix}$$

$$C = \begin{bmatrix} 1 & R_{CL} & 0 & 0 \\ 0 & -R_{Cf} & 1 & R_{Cf} \end{bmatrix} \quad y = \begin{bmatrix} v_L \\ v_O \end{bmatrix}$$

$$B_C = \begin{bmatrix} 0 & -\frac{1}{C_L} \\ 0 & \frac{R_{CL}}{L_L} \\ 0 & 0 \\ \frac{K_p}{L_f} & 0 \end{bmatrix} \quad x = \begin{bmatrix} v_{CL} \\ i_{LL} \\ v_{Cf} \\ i_{Lf} \end{bmatrix} \quad u = \begin{bmatrix} u_1 \\ i_O \end{bmatrix} \quad D = \begin{bmatrix} 0 & -R_{CL} \\ 0 & 0 \end{bmatrix}$$

where $K_p = -\frac{N_s V_i}{N_p C_m}$ $\quad L_L = L_{L1} + L_{L2}$ $\quad R_{LL} = R_{LL1} + R_{LL2}$

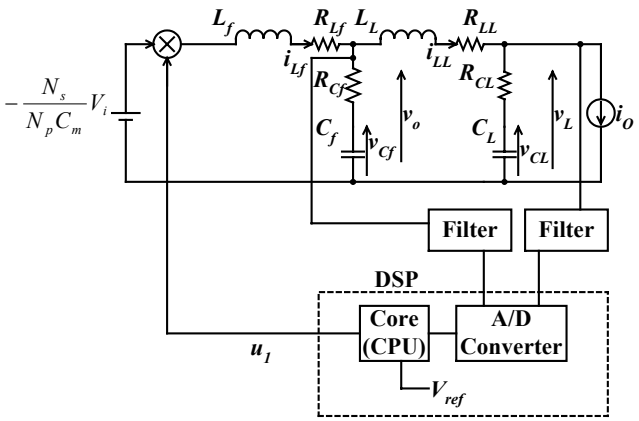

Fig. 2. Liner model of DC-DC converter

2.2 Response characteristics for controlled object

The response characteristics is investigated using the linear model of Fig. 2. From eq.(1), the transfer functions from u_1 and i_o to V_L become as follows:

$$\begin{aligned} W_{u1vL}(s) &= \frac{K_p L_L (1+sR_{Cf}C_f)(1+sR_{CL}C_L)}{g_4 s^4 + g_3 s^3 + g_2 s^2 + g_1 s + g_0} \\ W_{iovL}(s) &= \frac{h_4 s^4 + h_3 s^3 + h_2 s^2 + h_1 s + h_0}{g_4 s^4 + g_3 s^3 + g_2 s^2 + g_1 s + g_0} \end{aligned} \tag{2}$$

where

$$\begin{aligned} g_4 &= {L_L}^2 C_L L_f C_f \\ g_3 &= L_L C_L C_f \left[L_L (R_{Cf} + R_{Lf}) + L_f (R_{CL} + R_{LL} + R_{Cf}) \right] \\ g_2 &= L_L \begin{bmatrix} C_L C_f \left(R_{CL} R_{Cf} + R_{CL} R_{Lf} + R_{LL} R_{Cf} + R_{LL} R_{Lf} + R_{cf} R_{Lf} \right) \\ + C_L L_L + C_L L_f + C_f L_f \end{bmatrix} \\ g_1 &= L_L \left[C_L (R_{CL} + R_{LL} + R_{Lf}) + C_f (R_{Cf} + R_{Lf}) \right] \\ g_0 &= L_L \\ h_4 &= -R_{CL} g_4 \\ h_3 &= -L_L C_f \left\{ L_L L_f + C_L R_{CL} \left[L_L (R_{Cf} + R_{Lf}) + L_f (R_{CL} + R_{LL} + R_{Cf}) \right] \right\} \\ h_2 &= -L_L \begin{bmatrix} (L_L + L_f)(R_{Cf} C_f + R_{CL} C_L) + C_f (L_L R_{Lf} + L_f R_{LL}) + \\ R_{CL} C_L C_f (R_{CL} R_{Cf} + R_{CL} R_{Lf} + R_{Cf} R_{Lf} + R_{LL} R_{Cf} + R_{LL} R_{Lf}) \end{bmatrix} \\ h_1 &= -L_L \begin{bmatrix} L_L + L_f + C_f (R_{LL} R_{Cf} + R_{LL} R_{Lf} + R_{Lf} R_{Cf}) \\ + C_L R_{CL} (R_{CL} + R_{LL} + R_{Lf}) \end{bmatrix} \\ h_0 &= {R_{CL}}^2 C_L C_f L_f (R_{CL} + R_{LL} + R_{Cf}) + L_L (R_{LL} + R_{Lf}) \end{aligned}$$

Table 1. Parameters of controlled object

L_f	2.3 uH	R_{Lf}	20m Ω
L_L	0.1nH, 5uH	R_{LL}	3m Ω
C_f	21.6mF	R_{Cf}	2.125m Ω
C_L	21.6mF	R_{CL}	2.125m Ω
N_p	17 Turn	N_s	2 Turn
V_i	375 V	C_m	428

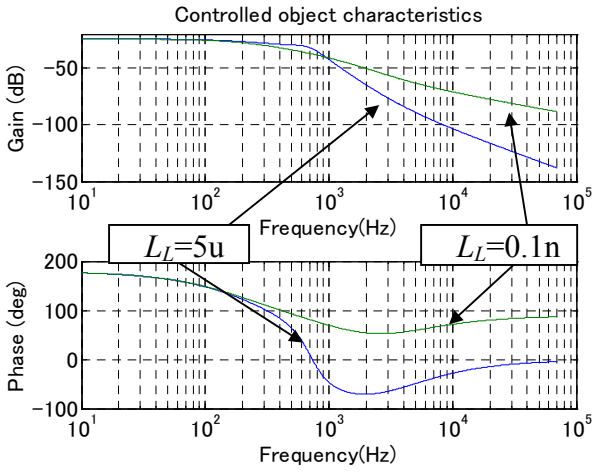

Fig. 3 Frequency characteristics of u_1-v_L

The frequency characteristic of u1-vL at the parameter of Table 1 is shown in Fig. 3. It turns out that as compared with L_L *=0.1nH,* at L_L*=5uH,* the phase characteristic changes

largely and the phase of the lowest point is falling by 180 degrees or more compared with low frequency range. Therefore, when a feedback control system is constituted, it turns out that the stbilization at L_L=*5uH* is difficult. Moreover, at high frequency, the gain characteristics at L_L=*5uH* is lower than the one at L_L=*0.1nH*. For this reason, it turns out that the compensation to the disturbance to v_L , such as load sudden change, is difficult. The frequency characteristics of i_o - v_L , i.e., the output impedance is shown in Fig. 4. From Fig. 4, it turns out that the output impedance will get worse if L_L becomes large, and it has a peak.

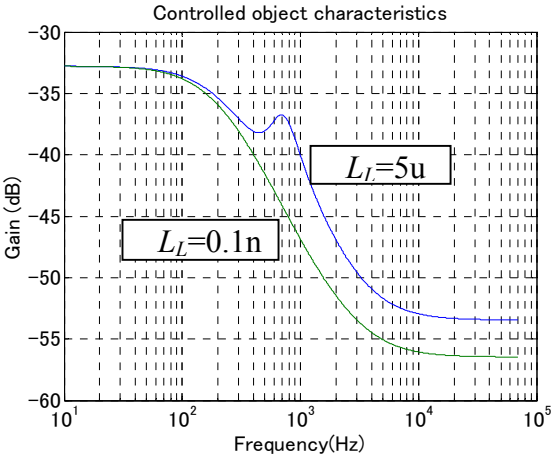

Fig. 4 Frequency characteristics of i_o-v_L (Output impedance)

3. CONTROLLER AT REMOTE SENSING

3.1 Digital robust controller

The continuous system of eq.(1) is transformed into the discrete system as follows:

$$x_d(k+1) = A_d x_d(k) + B_d u_d(k) \tag{3}$$

where

$$A_d = e^{AT} = I + AT + \frac{1}{2!}A^2T^2 + \frac{1}{3!}A^3T^3 + \cdots$$

$$B_d = A^{-1}(e^{AT} - I)B = TB + \frac{1}{2!}AT^2B + \frac{1}{3!}A^2T^3B + \cdots$$

$$x_d(k) = \begin{bmatrix} v_L(k) \\ i_{LL}(k) \\ v_O(k) \\ i_{Lf}(k) \end{bmatrix} \quad u_d(k) = \begin{bmatrix} u_1(k) \\ i_O(k) \end{bmatrix}$$

In order to compensate the delay by ADC conversion time and DSP operation time etc., a state ξ_1 is introduced, and a state ξ_2 is introduced for the current feedback equivalent conversion. Taking these into consideration, the control object is expanded as follows:

$$\begin{aligned} x_{d1}(k+1) &= A_{d1}x_{d1}(k) + B_{d1}u_{d1}(k) \\ y_{d1}(k+1) &= C_{d1}x_{d1}(k) \end{aligned} \tag{4}$$

where

$$A_{d1} = \begin{bmatrix} A_d & B_{du1} & 0 \\ 0 & 0 & 1 \\ 0 & 0 & 0 \end{bmatrix} \quad B_{d1} = \begin{bmatrix} 0 \\ 0 \\ 0 \\ 0 \\ 0 \\ 1 \end{bmatrix} \quad x_{d1}(k) = \begin{bmatrix} x_d(k) \\ \xi_1(k) \\ \xi_2(k) \end{bmatrix} \quad y_{d1}(k) = \begin{bmatrix} v_L(k) \\ v_O(k) \end{bmatrix}$$

$$C_{d1} = \begin{bmatrix} C_C & 0 & 0 \end{bmatrix} \quad B_{du1} = \begin{bmatrix} B_d(1,1) \\ B_d(2,1) \\ B_d(3,1) \\ B_d(4,1) \end{bmatrix} \quad u_{d1}(k) = u_2(k)$$

Here, in controller constitution, since input i_o is unnecessary, it has been deleted. To the system of eq.(3), the model matching control system using the state feedback is constituted as shown in Fig. 5. The system of Fig. 5 is described as follows:

$$\begin{aligned} x_{d2}(k+1) &= A_{d2}x_{d2}(k) + B_{d2}u_{d2}(k) \\ y_{d2}(k+1) &= C_{d2}x_{d2}(k) \end{aligned} \tag{5}$$

where

$$A_{d2} = \begin{bmatrix} & A_d & & & B_{du1} & 0 \\ f_b & C(1,2)f_b + C(2,2)f_d & f_d & C(2,4)f_d & 0 & 1 \\ f_a & C(1,2)f_a + C(2,2)f_c & f_c & C(2,4)f_c & f_e & f_f \end{bmatrix}$$

$$B_{d1} = \begin{bmatrix} 0 \\ 0 \\ 0 \\ 0 \\ G_H \\ G_G \end{bmatrix} \quad \begin{aligned} &C_{d2} = C_{d1} \quad x_{d2}(k) = x_{d1}(k) \\ &y_{d2}(k) = y_{d1}(k) \quad u_{d2}(k) = r(k) \end{aligned} \quad G_G = (f_f - H6)G_H$$

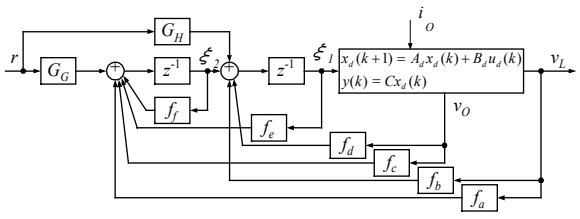

Fig. 5 Model matching system

From eq.(4), the transfer function from r to y becomes as follows:

$$\begin{aligned} W_{ry}(z) &= C_{d2}(zI - A_{d2})^{-1}B_{d2} \\ W_{ry}(z) &= \begin{bmatrix} W_{rvL}(z) \\ W_{rvO}(z) \end{bmatrix} \end{aligned} \tag{6}$$

where

$$\begin{aligned} &W_{rvL}(z) = K_{WrvL}\frac{N_{WrvL}(z)}{D_{WrvLmm}(z)} \\ &N_{WrvL}(z) = (z - H6)(z - n1)(z - n2)(z - n3) \\ &D_{WrvL}(z) = z^6 + F_5z^5 + F_4z^4 + F_3z^3 + F_2z^2 + F_1z + F_0 \\ &K_{WrvL} = G_H K_{u1vL} \end{aligned} \tag{7}$$

K_{u1vL} is the gain of the transfer function between v_1-v_L of eq.(3), and $n1$, $n2$ and $n3$ are the zeros of it. The transfer function of the system of Fig. 5 is specified as follows:

$$W_{rvLmm}(z) = K_{WrvLmm}\frac{N_{WrvL}(z)}{D_{WrvLmm}(z)}$$
$$N_{WrvL}(z) = (z-H6)(z-n1)(z-n2)(z-n3)$$
$$D_{WrvLmm}(z) = (z-H1)(z-H2)(z-H3)(z-H4)(z-H5)(z-H6)$$
$$K_{WrvLmm} = \frac{(1-H1)(1-H2)(1-H3)(1-H4)(1-H5)}{(1-n1)(1-n2)(1-n3)} \quad (8)$$

The state feedback coefficients f_a, f_b, f_c, f_d, f_e and f_f are decided to hold W_{rvL} (z) = W_{rvLmm} (z). If placing $H4$=$n1$, $H5$=$n2$ and $H1$>>$H2$, $H3$, W_{rvLmm} (z) will become an approximated first-order system and the following equation will be obtained.

$$W_{rvLmm}(z) \approx W_m(z) = \frac{1-H1}{z-H1} \quad (9)$$

The system added the system of eq.(9) and the following filter is constituted as shown in Fig. 6.

$$K(z) = \frac{k_Z}{z-1+k_Z} \quad (10)$$

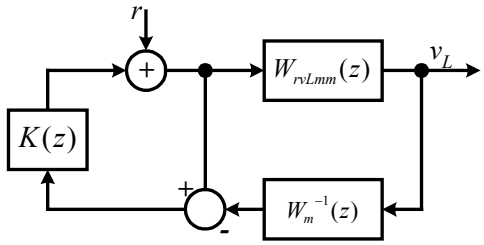

Fig. 6 Robust control system

If the system of Fig.6 is transformed equivalently, the integral type control system as shown in Fig. 7 will be obtained. Here f_{a1}, f_{b2}, K_i, K_{iz}, K_{r1}, and K_{r2} become as follows:

$$f_{a1} = -\frac{G_G k_z}{1-H1} + f_a \quad f_{b1} = -\frac{G_H k_z}{1-H1} + f_b$$
$$K_i = G_H k_z \quad K_{iz} = G_G k_z \quad (11)$$
$$K_{r1} = G_H \quad K_{r2} = G_G$$

In Fig. 7, the transfer functions from r to v_L and i_o to v_L become as follows:

$$W_{rvL}(z) \approx \frac{k_z}{z-1+k_z} \quad (12)$$

$$W_{iovL}(z) \approx \frac{z-1}{z-1+k_z} W_{iovLmo}(z) \quad (13)$$

Here W_{iovLmo} is the i_o -vL transfer function of the system of Fig. 5. From eqs.(12) and (13), it turns out that the characteristics from r to v_L can be specified with $H1$, and the characteristics from i_o and v_L can be independently specified with k_z . That is, the system of Fig.7 is an approximate 2DOF, and its sensitivity against the output impedance becomes lower with the increase of k_z.

3.2 Design of control system

The controller which satisfies the following specifications will be designed.

(1) Let the range of inductance L_L of the load lines be 0 μ H-5 μ H. And let the range of the load capacitor C_L be 3300 μ F-400mF. The control system is stable in the above-mentioned range.

(2)The output voltage change by load sudden change within all the frequency bands in the range of L_L in spec.(1) is less than (less than 20log(12[V]x0.03x2[Ω]/30[A]) =-32.4dB Ω) ±3%. Then it is possible to use the load capacitor C_L .

(3)The output voltage change by load sudden change within the frequency band 1kHz or less at L_L =0 μ H and C_L =0 μ H is less than (less than 20log(12[V]x0.03x2[Ω]/30[A]) = -32.4dB Ω) ±3%.

The control system is designed using L_L=0.5 μ H in the controlled object of Table.1 and the sampling period T_s = 14.3 μ s. First of all, the parameters Hi, i=1,…,6 are specified as follows:

$$H1 = 0.996,\ H2 = 0.78,\ H3 = 0.781$$
$$H4 = 0.7316,\ H5 = -0.7334,\ H6 = 0.01 \quad (14)$$

Next, how to determine k_z using the output impedance will be shown. The output impedance characteristics is derived from the control system of Fig. 7.

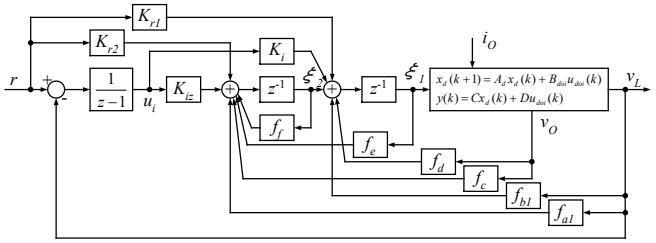

Fig, 7 The integral type control system

The output impedance characteristic is shown in Fig. 8. In this figure, R_{CL} is in inverse proportion to the value of C_L, and is R_{CL} =2.125(m Ω) x21.6(mF)/C_L,. The result of (a) and (c) is low impedance so that k_z is more large. On the other hand, the result of (b) is high impedance near 1kHz so that k_z is more large. From the these results, k_z is determined as k_z = 0.06. The output impedance characteristic when changing the load capacitor C_L from 1000 μ Fs to 400mFs is shown in Fig. 9. In this figure, C_L is made to increase every 2 times from 1000 μ F to 400mF (1000 μ F, 2000 μ F, 4000 μ F, --256mF, 400mF). Moreover, R_{CL} is in inverse proportion to the value of C_L and is R_{CL} =2.125(m Ω) x21.6(mF)/C_L . From this figure, it turns out that impedance can be reduced by making C_L increase to all L_L, and -40dB or less has been attained from the low to the high region.

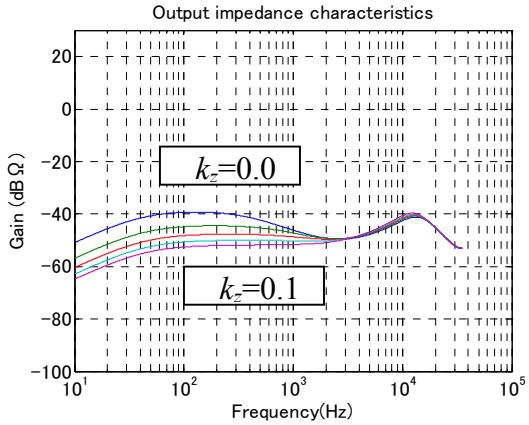

(a) L_L=0uH, C_L=0uF

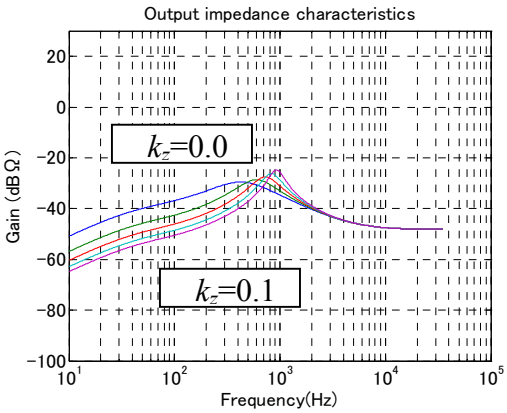

(b) L_L=5uH, C_L=1000uF

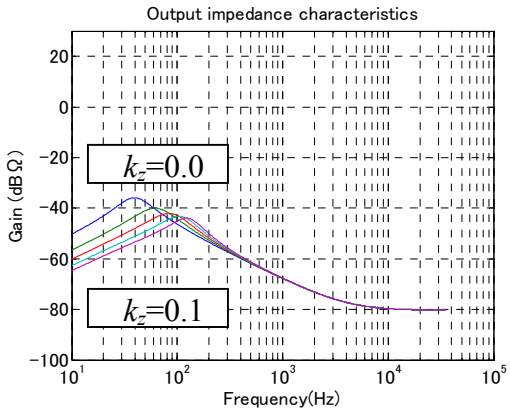

(c) L_L=5uH, C_L=400mF

Fig. 8 Output impedance characteristics

4. EXPERIMENTAL STUDIES

From eq.(13), the parameters of the system of Fig. 5 is determined as

$$f_a = -173,\ f_b = 164,\ f_c = -179,\ f_d = 325$$
$$f_e = 0.33,\ f_f = 0.28,\ GG = 1.05,\ GH = -3.9 \qquad (15)$$

From eq.(10), the parameters of the system of Fig. 7 is determined as

$$f_{a1} = -141,\ f_{b1} = 281,\ K_i = -0.467,\ K_{iz} = 0.126 \qquad (16)$$

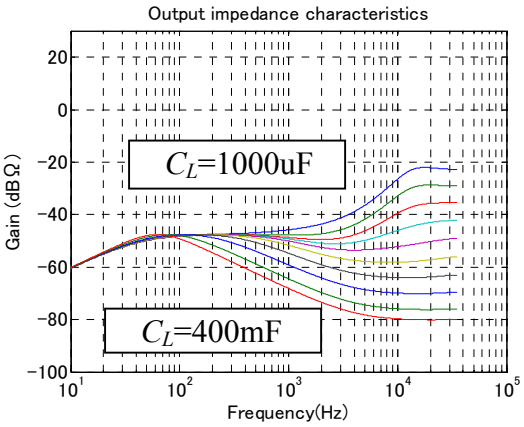

(a) L_L=0uH

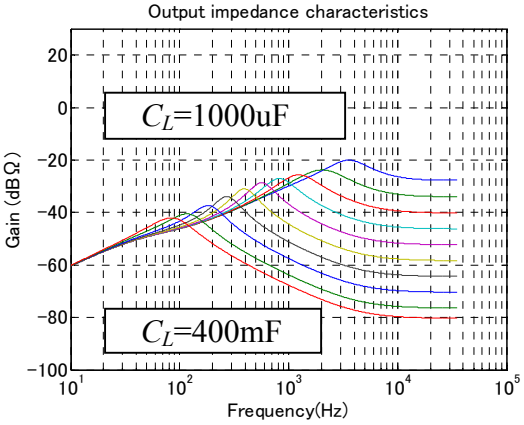

(c) L_L=5uH

Fig. 9 Output impedance characteristics

The simulation results at load sudden change are shown in Fig. 10. In this figure, R_{CL} is in inverse proportion to the value of C_L, and is R_{CL} =2.125(mΩ) x21.6(mF)/C_L . It turns out that even if the lines become long, if capacity is increased, the output voltage change will satisfy specification without oscillation. The experiment results at load sudden change is shown in Fig. 12. In this figure, the capacitor ELXZ250E332M (25V, 3300 μ F) by NIPPON CHEMI-CON CORP are used. This figure shows that the same result as simulations are obtained. The experiment results at load sudden change used usual controller PID is shown in Fig. 13. The output voltage across load is oscillated. By the proposed controller, it did not oscillate on the same conditions as this. As a result, it turns out that proposed one is effective practically.

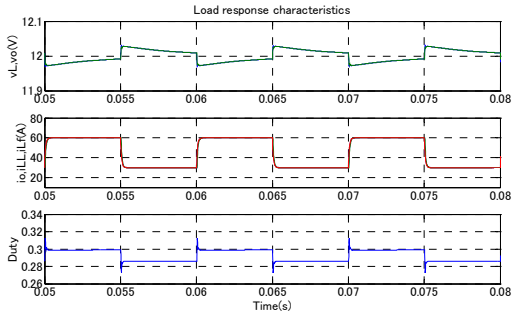

(a) L_L=0uH, C_L=0uF

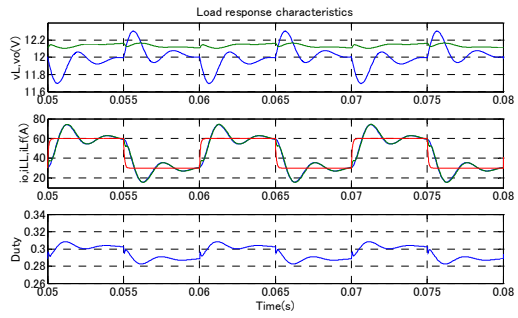

(b) L_L=5uH, C_L=33000uF

Fig. 10 The simulation results of load sudden change

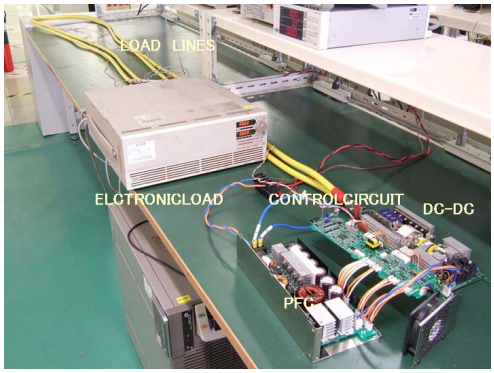

Fig. 11 The experimental system

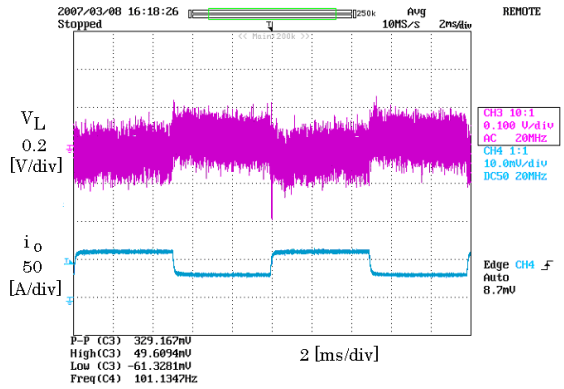

(a) L_L=0uH , C_L=0uF

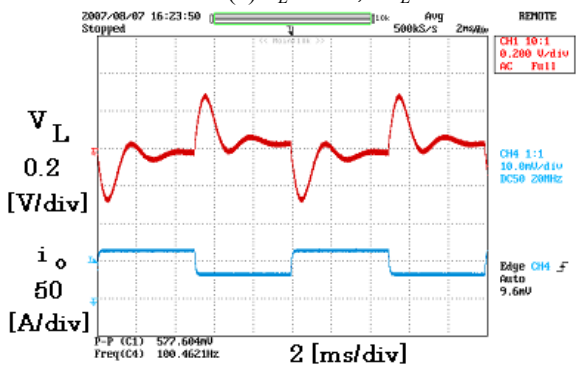

(b) Length of line=5m, C_L=33000uF

Fig. 12 The experimental results of load sudden change

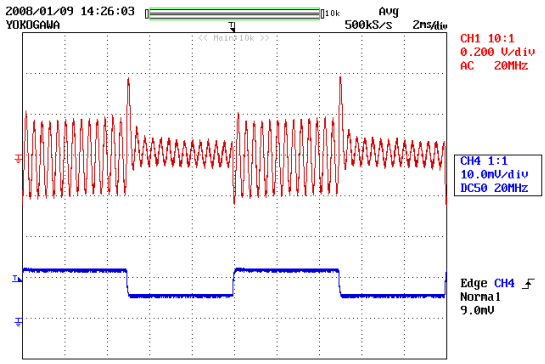

Fig. 13 The experimental results of load sudden change, where the controller is PID. Length of line=1m, C_L=6600uF

5. CONCLUSIONS

In this paper, the concept of controller of DC-DC converter with the long lines to attain good robustness against the changes of the voltage across load was given. The proposed digital controller was implemented on the DSP(TI TMS320LF2801). The DC-DC converter built-in this DSP was manufactured. It was shown from experiments that the proposed approximate 2DOF digital controller can suppress the change of voltage across load enough having no relation of the length of the lines. This fact demonstrates the usefulness and practicality of our proposed method.

REFERENCES

Guo, H., Shiroishi, Y. and Ichinokura, O. (2003). Digital PI Controller for High Frequency Switching DC/DC Converters Based on FPGA, *IEEE INTELEC'03,* pp.536-541.

Higuchi, K, Nakano, K, T.Kajikawa, T, Takegami, E., Tomioka, S., Watanabe, K. (2004). Robust Control of DC-DC Converter by High-Order Approximate 2-Degree-of-Freedom Digital Controller, *IEEE IECON'2004*, (CD-ROM).

Higuchi, K, Nakano, K, T.Kajikawa, T, Takegami, E., Tomioka, S., Watanabe, K. (2005). A New Design of Robust Digital Controller for DC-DC Converters, *IFAC 16th Triennial World Congress*, (CD-ROM).

Fukuda, H. and Nakaoka,, M. (1993). State-Vector Feedback Controlled-based 100kHz Carrier PWM Power Conditioning Amplifier and Its High-Precision Current-Tracking Scheme, *IEEE IECON'93,* pp.1105-1110.